Submitted to Nuclear Physics

LBL-2349
Preprint

RECEIVED
LAWRENCE
RADIATION LABORATORY

MAR 20 1974

LIBRARY AND
DOCUMENTS SECTION

DECOUPLED BANDS IN ODD-MASS MERCURY ISOTOPES

D. Proetel, D. Benson, Jr., A. Gizon, J. Gizon,
M. R. Maier, R. M. Diamond and F. S. Stephens

January 1974

Prepared for the U. S. Atomic Energy Commission
under Contract W-7405-ENG-48

TWO-WEEK LOAN COPY

This is a Library Circulating Copy which may be borrowed for two weeks. For a personal retention copy, call Tech. Info. Division, Ext. 5545

LAWRENCE BERKELEY LABORATORY
UNIVERSITY OF CALIFORNIA
BERKELEY

LBL-2349

DISCLAIMER

This document was prepared as an account of work sponsored by the United States Government. While this document is believed to contain correct information, neither the United States Government nor any agency thereof, nor the Regents of the University of California, nor any of their employees, makes any warranty, express or implied, or assumes any legal responsibility for the accuracy, completeness, or usefulness of any information, apparatus, product, or process disclosed, or represents that its use would not infringe privately owned rights. Reference herein to any specific commercial product, process, or service by its trade name, trademark, manufacturer, or otherwise, does not necessarily constitute or imply its endorsement, recommendation, or favoring by the United States Government or any agency thereof, or the Regents of the University of California. The views and opinions of authors expressed herein do not necessarily state or reflect those of the United States Government or any agency thereof or the Regents of the University of California.

NUCLEAR REACTIONS: $^{194,195,196,198}Pt(\alpha,xn)^{195,197,199}Hg$; x = 3,4. E_α = 34 - 50 MeV, measured $\sigma(E_\gamma,\theta)$, $^{195,197,199}Hg$ deduced levels, J, π. Enriched targets, Ge(Li) detectors.

DECOUPLED BANDS IN ODD-MASS MERCURY ISOTOPES*

D. Proètel†, D. Benson, Jr.‡, A. Gizon‡‡, J. Gizon‡‡, M. R. Maier‡‡‡,
R. M. Diamond and F. S. Stephens

Lawrence Berkeley Laboratory
University of California
Berkeley, California 94720

January 1974

Abstract

The schemes of the low-lying high-spin states in mercury isotopes with A = 195, 197, and 199 have been studied by γ-ray spectroscopy following (α,xn) reactions on separated platinum targets. Two bands have been excited in each Hg nucleus, one with positive parity based on the isomeric $i_{13/2}$ state and one, probably with negative parity, starting at spin 21/2. The positive-parity states are interpreted within the rotation-aligned coupling scheme as decoupled bands, this implies oblate deformation in these three Hg isotopes. The negative-parity states are discussed as a decoupled $i_{13/2}$ neutron state coupled to the 5^-, 7^-, 9^-, • • • states, recently discovered in even-even mercury isotopes.

*Work performed under the auspices of the U. S. Atomic Energy Commission.

†On leave from: Sektion Physik der Universität München, 8046 Garching, West Germany.

‡Present address: Brookhaven National Laboratory, Upton, New York 11973.

‡‡Present address: Institut des Sciences Nucleaires, BP 257, Grenoble 38044, France.

‡‡‡Present address: Physik Department der TU München, 8046 Garching, West Germany.

1. Introduction

The occurrence of a low-lying $13/2^+$ level in odd-A mercury isotopes is well known, and these states have been identified as the unique-parity $i_{13/2}$ neutron-hole states. This interpretation seems reasonable at first because the Nilsson diagram shows that the $\Omega = 13/2$ substate is - for prolate deformation - upsloping and lies close to the Fermi surface at reasonably small deformations ($\beta \approx 0.15$). But in recent measurements a trend from prolate to oblate deformation has been discovered in Os and Pt nuclei[1]). Also in ^{199}Tl and some odd-Au isotopes evidence for oblate deformation has been found[2-4]). Assuming that this trend continues into the Hg nuclei, the existence of a low-lying $13/2^+$ state is no longer easy to understand in the usual strong-coupling scheme; the $\Omega = 13/2$ state lies quite far below the Fermi surface for oblate deformation. In this case it is the $\Omega = 1/2$ state which comes close to the Fermi surface, and this is the situation in which a new coupling scheme has recently been predicted to be valid: the rotation-aligned coupling scheme[5,6]). In this coupling scheme an odd particle moving in a high-j orbital with a small projection Ω on the symmetry axis of the nucleus is - due to the Coriolis force acting on it - decoupled from the nuclear symmetry axis and aligned along the nuclear rotation axis. The excited states built in the two coupling schemes are very different; whereas the energies of the states in the strong-coupling scheme are in the simplest approximation proportional to $I(I+1)$ with a spin sequence of I, I+1, I+2, and so on, one expects in the rotation-aligned scheme so-called decoupled bands, with states having spins $I = j, j+2, j+4, \cdots$ separated by energies equal to the $2^+ \rightarrow 0^+$, $4^+ \rightarrow 2^+$

$6^+ \rightarrow 4^+$, ··· transition energies in the adjacent even-even core nuclei. (For the states with spin I+1, I+3, I+5, ···, the odd particle is not fully aligned, and one expects these states at higher excitation energies.) These very different spectra make it easy to distinguish which of the coupling schemes applies in a particular case.

In the present paper we report on the discovery of decoupled bands built on the $13/2^+$ state in the odd-A mercury isotopes with A = 195, 197, and 199, by means of in-beam γ-ray spectroscopy. This implies oblate deformation for these three Hg isotopes, because only then are the low Ω orbits of the $i_{13/2}$ subshell close to the Fermi surface so that the rotation-aligned coupling scheme should apply.* Moreover, we find states in these three nuclei which appear to consist of a decoupled $i_{13/2}$ neutron coupled to the 5^-, 7^-, 9^-, ··· states previously known in the even-even Hg nuclei[8]).

*Preliminary results have been published in an earlier publication[7]).

2. Experimental Techniques

The mercury nuclei with A = 195, 197 and 199 have been studied using γ-ray spectroscopy following (α,xn) reactions on self-supporting enriched platinum targets of approximately 5 mg/cm^2 thickness. Two Pt targets have been used with relative abundances of 60% ^{198}Pt, 30% ^{196}Pt, 10% ^{195}Pt, and 60% ^{194}Pt, 30% ^{195}Pt, 10% ^{196}Pt. Excitation functions for the (α,3n) and (α,4n) reactions have been studied at seven different energies between 34 and 50 MeV, with α beams provided by the 88" cyclotron of the Lawrence Berkeley Laboratory. The time structure of the cyclotron beam (pulse width ∿ 10 nsec, distance between beam pulses ∿ 150 nsec) was used to accumulate in-beam and off-beam spectra in order to determine isomeric transitions and short-lived activities[9]). The anisotropies of the γ-ray angular distributions have been measured at 45° and 90° in the reaction plane. Conventional fast-slow coincidence techniques were used to record γ-γ coincidences between a planar and a coaxial Ge(Li) detector, both located at 90° with respect to the incident beam. In the coincidence runs the beam energy was 37 MeV in the bombardment of the Pt target with the heavier mass composition and 40 MeV in the bombardment of the lighter one. The relative efficiencies of the Ge(Li) detectors were determined with ^{177m}Lu and ^{152m}Eu sources.

3. Experimental Results

In the (α,3n) and (α,4n) reactions leading to the Hg isotopes with A = 195, 197, and 199 well established band structures are heavily populated. Up to five γ transitions have been observed in a cascade and their 45°/90° intensity ratio is fully consistent with stretched E2 multipolarity. We have evidence that this band structure is based on the $13/2^+$ isomeric states in each Hg nucleus. This evidence consists of a comparison of the production of the $13/2^+$ state with the yield of the lowest transition in the excited band. It has been determined that in ^{199}Hg and in ^{197}Hg this transition accounts for about one-half of the production of the $13/2^+$ isomeric state. Almost all the stronger γ-lines which were identified (from excitation functions) as transitions in the odd-A Hg nuclei are in prompt (within a few nsec) coincidence with this transition. The decay schemes for the high-spin states have been determined mainly from the γ-γ coincidence measurements. From the anisotropies of the γ ray transitions, measured at 45° and 90° in the reaction plane, and with the assumption that $A_4 = 0$ (for most of the cases this only introduces a small error) approximate A_2 coefficients for the angular distributions were derived. Since the decay of all the transitions assigned to the three odd-A isotopes is faster than a few nanoseconds, we assume that their multipolarity is either electric quadrupole or magnetic or electric dipole. Positive A_2 coefficients around 0.4 were assigned to stretched ($I \rightarrow I-2$) E2 or non-stretched ($I \rightarrow I$) M1 or E1 transitions. Unfortunately, the accuracy of our data does not allow us to distinguish between these types of multipolarities; however, in some cases the spin of a

level could be assigned unambiguously from its branched decay to other known levels. Some of the γ rays show a very sharp 90°-peaked angular distribution ($A_2 \lesssim -0.5$). With the restriction to $\ell = 1$ and 2, they can only be produced by mixed quadrupole/dipole transitions of the type $I\pm1 \rightarrow I$ with a mixing ratio $\delta = \langle I|M(L2)|I\pm1\rangle / \langle I|M(L1)|I\pm1\rangle \approx \mp1$. Since M2/E1 transitions with this mixing ratio seem to us very unlikely, we assign them as E2/M1 transitions. It will be shown in Sec. 4 that in the rotation-aligned model, one predicts a negative (positive) value for the E2/M1 mixing ratio for the decay of a class of states of the type $I+1 \rightarrow I$ ($I-1 \rightarrow I$) in these Hg nuclei. Furthermore, we used the general rules that - as is typical in (HI,xn) reactions - the population of the states decreases and the spin of the levels generally increases as one goes up in excitation energy in a nucleus; and also, that the population of the high-spin states increases relative to that of the low-spin states as the bombarding energy is increased. From these arguments, γ rays with sharp 90°-peaked angular distributions are assigned as $I+1 \rightarrow I$ transitions of mixed E2/M1 multipolarity.

In the following, we present the arguments which led us to the decay schemes of the low-lying high-spin states in the three nuclei, ^{195,197,199}Hg. The relative intensities and approximate A_2 coefficients for the transitions assigned to these nuclei are given in Tables 1, 3 and 4, respectively. Although we are dealing with odd nuclei near the closed proton and neutron shells, the spectra of the odd-A Hg nuclei are relatively simple and remarkably similar to those of the adjacent even-even Hg nuclei. We observe a positive-parity band based on the $13/2^{+}$ state connected with stretched E2 transitions, and a

presumably negative-parity band starting at $21/2^-$ which decays into the positive-parity band around spin $21/2^+$. Because of this simplicity, we will not discuss the decay of each individual level; the decay schemes follow quite straightforwardly from the coincidence data. Figure 1 displays two γ-spectra recorded at 90° from $^{194,(195)}$Pt bombarded with α particles of 35 MeV and 45 MeV. Figure 2 is a similar spectrum from $^{(196),198}$Pt at 34 MeV α energy and 90°, with the insert showing the higher γ-energies at 45°. It can be seen that some of the lines (741.5 keV and 945.3 keV) are almost absent at 45°. In fig. 3 we show some coincidence spectra on ^{199}Hg in order to give an impression of their quality.

3.1. ^{195}Hg

As we have discussed above, the observed band structure very likely feeds the $13/2^+$ isomeric state. The low γ ray energies make the determination of the intensity balance of the $17/2^+ \rightarrow 13/2^+$ transition versus the production of the $13/2^+$ activity difficult in this case, so this conclusion has been drawn by analogy to ^{197}Hg and ^{199}Hg where these intensity balances could be determined. From the coincidence measurement, a cascade of five γ-rays, 371.2 keV, 611.6 keV, 710.1 keV, 544.7 keV, and 278.4 keV (listed in the order of decreasing relative intensity), is well established. The A_2 coefficients of these transitions are around +0.45 ± 0.10, which is typical for stretched E2 transitions and, in the excitation function studies, the relative population of the higher excited states increases at higher bombarding energies relative to the population of the lower excited states, indicating that the spin increases up the cascade. These arguments lead to a band with the following

states: $17/2^+$ at 547.3 keV, $21/2^+$ at 1158.9 keV, $25/2^+$ at 1869.0 keV, $29/2^+$ at 2413.7 keV and $33/2^+$ at 2692.1 keV. The coincidence measurements show another cascade of three γ-rays, 586.2 keV, 125.7 keV, 301.1 keV (listed in the order of decreasing intensity), which enters the previously described band at the $21/2^+$ state. This leads to levels at 1744.8 keV, 1870.5 keV and 2171.6 keV. The 1744.8 keV level branches off via a 283.4 keV transition to a state at 1461.1 keV, which decays with a 913.8 keV γ ray to the $17/2^+$ level at 547.3 keV. The 913.8 keV γ ray is one of the sharp 90°-peaked transitions of mixed E2/M1 multipolarity of the type I+1 → I (see Sec. 4). This identifies the level at 1461.1 keV as a $19/2^+$ state. The assignment of spin 21/2 for the level at 1744.8 keV is the only possibility which is consistent with the anisotropies measured for the γ rays of its decay to the $19/2^+$ state at 1461.1 keV and to the $21/2^+$ state at 1158.9 keV. The two γ rays of 125.7 keV and 301.1 keV which are in cascade with each other and which feed the level at 1744.8 keV have anisotropies characteristic for stretched quadrupole multipolarity. This implies a spin of 25/2 for the level at 1870.5 keV and 29/2 for the level at 2171.6 keV. Unfortunately, we cannot prove unambiguously the parities of these three states; however, intensity balances of the 283.4 keV line versus the 913.8 keV line favors an E1 assignment for the 283.4 keV transition. Table 2 lists the intensities (corrected for angular distribution and relative to the $17/2^+ \rightarrow 13/2^+$ transition, which has been set equal to 100) for the two lines at various bombarding energies from E_α = 34 MeV up to E_α = 50 MeV. At the lower α energies, the 283.4 keV line is clearly the weaker transition, placing the 913.8 keV line lower in the decay scheme. But

at the high α energies the intensity of the 283.4 keV line approaches that of the 913.8 keV line. The conversion coefficients for a 283 keV transition are 0.44 for M1, 0.12 for E2 and 0.03 for E1 multipolarity. Therefore, pure M1 multipolarity seems unlikely because this would make the total transition intensity of the 283.4 keV line stronger than that of the following 913.8 keV line at the high bombarding energies. An E2 multipolarity (implying positive parity for the 21/2 state) also seems to us unlikely because of the absence of a transition to the $17/2^+$ state at 547.3 keV. From these arguments we believe that a parity change is involved in the 283.4 keV and 586.2 keV transitions, which implies negative parity for the states at 1744.8 keV (21/2), 1870.5 keV (25/2) and 2171.6 keV (29/2). We identify these levels as states based on an $i_{13/2}$ neutron coupled to the negative-parity 5^-, 7^-, and 9^- states, which have been observed in the even-even Hg nuclei[8]). This point will be discussed in more detail in Sec. 4. The $19/2^+$ state is, we believe, an unfavored state of the positive-parity band, which has been shifted up in energy because it is less favored by the Coriolis interaction. Two γ-rays of 121.4 keV and 214.8 keV which belong - according to the excitation function measurements and the coincidence experiments - to ^{195}Hg could not be assigned. They seem to feed somewhere into the negative-parity states. Figure 4 shows the decay scheme of the states discussed above.

3.2. ^{197}Hg

Our information on ^{197}Hg comes from the (α,3n) data on ^{196}Pt, which was 30% abundant in the target with the heavier isotopic composition. Consequently, only the stronger γ-transitions could be assigned. Again we have a relatively simple structure of two bands, and at E_α = 37 MeV the intensity

of the lowest transition in the band is found to be ≈ 0.5 of the total activity of the $i_{13/2}$ state ($t_{1/2}$ = 23.8 h). Therefore, we conclude that the observed cascades terminate at the $13/2^+$ state. The coincidence data show one cascade of three γ transitions, 354.1 keV, 621.0 keV, and 763.1 keV, leading to levels at 653.1 keV, 1274.1 keV and 2037.2 keV. The other sequence of γ-rays, 408.2 keV, 150.7 keV and 328.6 keV, enters the former band at the 1274.1 keV level, indicating states at 1682.3 keV, 1833.0 keV and 2161.6 keV. Although the intensity of the 408.2 keV line is somewhat obscured in the singles spectra by the inelastic excitation of the 2^+ state in ^{198}Pt (407.2 keV), the level ordering could be determined rather unambiguously from a careful study of the intensities of the lines in the excitation function measurements and in the coincidence spectra.

The 354.1 keV, 621.0 keV and 763.1 keV γ-rays have anisotropies characteristic for stretched quadrupole transitions, so we conclude that they deexcite states of the positive-parity band with spin $17/2^+$ at 653.1 keV, $21/2^+$ at 1274.1 keV and $25/2^+$ at 2037.2 keV. These assignments also seem to us reasonable from the relative population of the states in the (α,xn) reaction and from the excitation function studies. To the levels at 1682.3 keV, 1833.0 keV and 2161.6 keV we tentatively assign spins of $21/2^-$, $25/2^-$ and $29/2^-$ by analogy to similar levels in ^{195}Hg. The observed anisotropies of the γ rays deexciting these states are fully consistent with these assignments. The positive A_2 coefficient of the 408.2 keV line (the $21/2^- \rightarrow 21/2^+$ transition) could, of course, also be interpreted as another stretched E2 transition. This would lead to a second positive parity band starting with spin $25/2^+$ which seems to us unlikely. The proposed scheme can be seen in fig. 5.

3.3. ^{199}Hg

Fifteen γ transitions could be assigned to a rather complex structure of two bands based on the $i_{13/2}$ state in ^{199}Hg. In this case, the intensity of the lowest transition in the band accounts (for the (α,3n) reaction at E_α = 37 MeV) for 0.6 of the formation of the isomeric $13/2^+$ state ($t_{1/2}$ = 42.6 min). From the coincidence data, the level scheme presented in fig. 6 has been determined. The anisotropies and excitation functions of the 291.4 keV, 533.5 keV and 749.9 keV lines led to the conclusion that they depopulate the states of a positive-parity band with a $17/2^+$ state at 832.9 keV, a $21/2^+$ state at 1357.4 keV and a $25/2^+$ state at 2107.3 keV. Three γ rays (741.5 keV, 945.2 keV, and 1126.6 keV) have sharp 90°-peaked angular distributions which we interpret as mixed E2/M1 transitions of the type ($I\pm1 \rightarrow I$). The 741.5 keV line does not show any other line coincident with it, so we place it directly feeding the isomeric $13/2^+$ state, depopulating a $15/2^+$ state at 1274.0 keV. The 945.2 keV γ ray feeds the $17/2^+$ level at 832.9 keV, and the 1126.6 keV line goes to the $21/2^+$ level at 1357.4 keV, leading to a $19/2^+$ state at 1778.1 keV and a $23/2^+$ state at 2484.0 keV. We interpret them as the unfavored positive-parity states which are not lowered in energy so much by the strong Coriolis interaction. In addition, we found six more states which we interpret as a negative-parity band starting at spin $21/2^-$. This band decays into the positive-parity band through four transitions. The anisotropies and excitation functions of the various γ-rays are fully consistent with these assignments; however, other assignments may also be possible, so our interpretation of this negative-parity band is tentative.

4. Discussion

We found the spectra of the high-spin states of ^{195,197,199}Hg to consist of two bands, a positive-parity one starting with spin 13/2 and a (probably) negative-parity one starting with spin 21/2. Figure 7 displays all available data on the 2^+, 4^+ and 6^+ states for even-even mercury nuclei and the $13/2^+$, $17/2^+$ and $21/2^+$ states in the odd-A mercury isotopes (solid bars) and the 5^-, 7^-, and 9^- states together with the $21/2^{(-)}$, $25/2^{(-)}$ and $29/2^{(-)}$ states (broken bars) in the even-even and odd-A nuclei. (The spectra of the odd-A nuclei have been shifted so that the $13/2^+$ states match up with the 0^+ states in the even-even Hg nuclei.) A striking regularity is apparent in the 2^+, 4^+, and 6^+ states and the corresponding $13/2^+$, $17/2^+$ and $21/2^+$ states through a range of 14 neutron numbers. Clearly, decoupled bands are occurring in the odd-A Hg nuclei with spin sequences 13/2, 17/2 and 21/2 and energies very similar to the core energies in the even-even Hg isotopes. In the context of the rotation-alignment model this implies oblate deformation for these nuclei, since for $\beta < 0$ the low Ω states of the $i_{13/2}$ subshell are close to the Fermi surface. For prolate deformation, one would expect a normal rotational band based on the $13/2^+$ state, with the usual spin sequence and energies approximately proportional to I(I+1). At the neutron-rich side in fig. 7 the decoupled states become gradually, but systematically, lower in energy than the corresponding core states. This behavior is not yet fully understood; it may be a shell effect (^{200}Hg also has a 2^+ state lower than the other Hg isotopes). At the extreme neutron-deficient side, the quasi-rotational ground band collapses rather suddenly due to the onset of strong deformation[10]); however, ^{187}Hg still seems to have a decoupled $21/2^+$ state.

Another interesting feature in these odd-A mercury isotopes is that some states can be identified as the unfavored states of the decoupled band (the $19/2^+$ state in ^{195}Hg and the $(15/2^+)$, $19/2^+$ and $23/2^+$ states in ^{199}Hg). For these states, the odd particle moving in the $i_{13/2}$ orbit is not fully aligned ($\alpha = 11/2$ instead of $\alpha = 13/2$, where α is the projection of j on I). The core rotating in higher spin states then yields, in a simplified picture, the spins of $15/2^+$, $19/2^+$ and $23/2^+$. The large energy spacings between the $15/2^+$ and $17/2^+$, $19/2^+$ and $21/2^+$, and $23/2^+$ and $25/2^+$ states indicates the inadequacy of considering these levels as weak-coupling multiplets. To a good approximation the wave functions of the aligned states can be written:

$$\psi^{Ij}_{M\alpha} \approx \sum_{\Omega} d^{j}_{\alpha\Omega}(\tfrac{\pi}{2})\, \chi^{j}_{\Omega}\, \mathcal{D}^{I}_{M\Omega} \quad , \tag{1}$$

where j is the spin of the particle, Ω its projection on the symmetry axis and α its projection on the rotation axis of the nucleus. Each state with fixed value of α is written as a sum over all Ω values with the amplitudes given by the function $d^{j}_{\alpha\Omega}(\frac{\pi}{2})$. These amplitudes are listed for the $\alpha = 13/2$ and $\alpha = 11/2$ states in Table 5. In eq. (1) χ^{j}_{Ω} represents the intrinsic Nilsson wave function of the particle and $\mathcal{D}^{I}_{M\Omega}$ describes the rotation of the entire system.

In the following, we want to derive a simple rule for the mixing ratio for E2/M1 transitions from a state $|I\pm1, \alpha = 11/2\rangle$ to a state $|I; \alpha = 13/2\rangle$, e.g. for transitions from the incompletely aligned states to the fully aligned states. The former ones are always raised in energy so these transitions should occur rather commonly. The E2 matrix element is proportional to

$$\langle I \| E2 \| I\pm 1 \rangle \sim Q_o \sum_{\Omega} \langle I\pm 1\ 2\ \Omega\ 0 | I\ \Omega \rangle\ d^{j}_{j-1,\Omega}(\tfrac{\pi}{2})\ d^{j}_{j\Omega}(\tfrac{\pi}{2}) \quad . \tag{2}$$

The non-diagonal matrix elements can be neglected, because they have only single-particle strength, whereas the diagonal matrix elements have the full collective strength. The sign of this matrix element is determined by the signs of Q_o and the Clebsch-Gordan coefficients. As discussed above, we have oblate deformation in the odd mercury isotopes resulting in a negative Q_o. All the Clebsch-Gordan coefficients are negative for the $I+1 \rightarrow I$ case and positive for the $I-1 \rightarrow I$ case.

In evaluating the M1 matrix element, we follow the procedure given in ref. [11]:

$$\begin{aligned} \langle I \| M1 \| I\pm 1 \rangle \sim \sum_{\Omega,\Omega'} d^{j}_{j-1,\Omega}(\tfrac{\pi}{2})\ d^{j}_{j,\Omega'}(\tfrac{\pi}{2})\ \big[& \langle I\pm 1\ 1\ \Omega\ \Omega'-\Omega | I\Omega' \rangle\ GM1(\Omega\rightarrow\Omega') \\ & + (-)^{I+\Omega'} \langle I\pm 1\ 1\ \Omega\ -\Omega'-\Omega | I\ -\Omega' \rangle\ GM1(\Omega\rightarrow -\Omega') \big] \end{aligned} \tag{3}$$

with

$$GM1(\Omega\rightarrow\Omega') = (g_s-g_R)GMS(\Omega\rightarrow\Omega') + (g_\ell-g_R)GML(\Omega\rightarrow\Omega') \quad .$$

For a neutron (hole) state, one uses $g_s \approx 0.6\ g_s(\text{free}) = -2.3$; $g_R \approx Z/A \approx 0.4$ and $g_\ell = 0$; the matrix elements GMS and GML are listed in ref. [11]. In this case one has to sum over all values of $\Omega' = \Omega$ and $\Omega' = \Omega\pm 1$. For both kinds of transitions ($I+1 \rightarrow I$ and $I-1 \rightarrow I$) eq. (3) gives negative M1 matrix elements.

These results seem to be valid rather generally and quite independently of the spin j of the particle, since the Clebsch-Gordan coefficients, the amplitudes of the wave functions, and the M1 matrix elements all change only gradually with changes in the value of j. Together with the sign of the E2 matrix element, this yields positive δ for the $I-1 \rightarrow I$ and negative δ for the $I+1 \rightarrow I$ transition, resulting in a negative A_2 coefficient in both cases. For an odd proton (the g-factors change their sign) <u>or</u> prolate deformation ($Q_o > 0$) the opposite sign for the mixing ratios and A_2 values is predicted, whereas for an odd proton <u>and</u> prolate deformation the same rules should apply.

The discovery of a (probably) negative-parity band with spin $21/2^-$, $25/2^-$ and $29/2^-$ states throws some light on the 5^-, 7^-, 9^-, ··· bands found in the even-even Hg isotopes, in the nearby Pb and Pt isotopes, and also near the closed N = 82 sheel. Clearly, the systematic occurrence and the enhanced transition probabilities ($\approx$ 30 s.p.u.) indicate some collective character for these states. On the other hand, the occasional very close spacings (5^- to 7^- in the case of the Hg nuclei) can be explained as a single-particle effect as has been discussed for the Pb isotopes[12,13]. These states probably have mainly two-neutron configurations, $(i_{13/2} \otimes p_{3/2})$, $(i_{13/2} \otimes p_{1/2})$ and $(i_{13/2} \otimes f_{5/2})$ where the nucleon-nucleon interaction - attractive in the singlet even state - brings those states lowest for which the overlap of the spatial wave functions of the two particles is maximal. These are the states with natural parity: 5^- and 7^- for $(i_{13/2} \otimes p_{3/2})$; 7^- for $(i_{13/2} \otimes p_{1/2})$; and 9^-, 7^-, and 5^- for $(i_{13/2} \otimes f_{5/2})$. The collectivity of the bands originates from two effects: 1) strong mixing of the states belonging to

multiplets, and 2) coupling of these two-particle states to the $I = 0^+, 2^+, 4^+, \cdots$ core states. The assumption that the negative-parity bands are built mainly on two-neutron (hole) states with one neutron decoupled ($\alpha = 13/2$) in the $i_{13/2}$ orbit, gets strong support from the occurrence of similar states ($21/2^-$, $25/2^-$, $29/2^-$) in the odd-A nuclei. The coupling of an $\alpha = 13/2$ neutron hole with the 5^-, 7^- and 9^- states would naively result in $23/2^-$, $27/2^-$ and $31/2^-$ states, but since the Pauli principle forbids two particles in the same $\alpha = 13/2$ orbit, one particle can only be partially aligned ($\alpha = 11/2$), leading to the observed spins of $21/2^-$, $25/2^-$ and $29/2^-$. If the $i_{13/2}$ neutron hole were not involved in the negative parity 5^-, 7^- and 9^-, $\cdots$ states, then one would expect to see spin sequences of $23/2^-$, $27/2^-$ and $31/2^-$.

5. Conclusion

In-beam γ ray spectroscopy following (α,xn) reactions on Pt isotopes has provided evidence for decoupled bands in odd-A mercury isotopes. Some of the unfavored states (α = 11/2) also seem to be seen, and their excitation energies follow qualitatively the predictions of the rotation-aligned coupling scheme. This provides additional evidence that this new coupling scheme may be a useful description for the low-lying high-spin states in these nuclei, and the large differences in energy between members of the multiplets show that weak-coupling schemes are invalid here. These results also indicate oblate deformation for the mercury isotopes as has been found in nearby Pt-, Au-, and Tl-isotopes. It appears that the strongly deformed (prolate) rare-earth region and the spherical lead region are connected by a transitional region with oblate deformation.

The observation of a probably negative-parity band in the odd-A mercury nuclei, starting at spin 21/2, strongly suggests that the excitation of a (decoupled) $i_{13/2}$ neutron hole plays a major role in the 5^-, 7^-, 9^-,··· bands recently discovered in the even-even mercury isotopes.

Acknowledgments

We would like to thank Dr. M. Redlich for valuable discussions. D.P. gratefully appreciates a grant from the University of Munich which made his stay at the Lawrence Berkeley Laboratory possible. J.G. appreciates support from a NATO fellowship. We also thank the crew of the 88" cyclotron for providing the α beams.

References

1. J. E. Glenn, R. J. Pryor, and J. X. Saladin, Phys. Rev. 188 (1969) 1905
2. J. O. Newton, S. D. Cirilov, F. S. Stephens, and R. M. Diamond, Nucl. Phys. A148 (1970) 593
3. K. Nakai, Phys. Letters 34B (1971) 269
4. F. S. Stephens, R. M. Diamond, D. Benson, Jr., and M. R. Maier, Phys. Rev. C7 (1973) 2163
5. J. R. Leigh, K. Nakai, K. H. Maier, F. Pühlhofer, F. S. Stephens, and R. M. Diamond, Nucl. Phys. A213 (1973) 1
6. F. S. Stephens, Rev. Mod. Phys., in press
7. D. Proetel, D. Benson, M. R. Maier, R. M. Diamond, and F. S. Stephens, Proceedings of the International Conference on Nuclear Physics, Munich (1973), ed. J deBoer and H. J. Mang, p. 194
8. R. F. Petry, R. A. Naumann, and J. S. Evans, Phys. Rev. 174 (1968) 1441
9. A more detailed description of the experimental details can be found in; J. Gizon, A. Gizon, M. R. Maier, R. M. Diamond and F. S. Stephens, submitted to Nucl. Phys.
10. D. Proetel, R. M. Diamond, P. Kienle, J. R. Leigh, K. H. Maier, and F. S. Stephens, Phys. Rev. Letters 31 (1973) 896; N. Rud, D. Ward, H. R. Andrews, R. L. Graham, and J. S. Geiger, Phys. Rev. Letters 31 (1973) 1421; and D. Proetel, R. M. Diamond, and F. S. Stephens, Phys. Letters 48B (1974) 102.
11. E. Browne and F. R. Femenia, Nucl. Data Tables 10 (1971) 81
12. M. Pautrat, G. Albouy, J. C. David, J. M. Lagrange, N. Poffé, C. Roulet, H. Sergolle, J. Vanhorenbeeck, and H. Abou-Leila, Nucl. Phys. A201 (1973) 449.
13. M. Redlich, private communication.
14. W. F. Davidson, private communication.

Table 1. Information on γ-Transitions Assigned to ^{195}Hg.

E_γ (keV)	I_γ at 47 MeV	A_2	Mult.	$E_x(i)$ (keV)	I(i)	$E_x(f)$ (keV)	I(f)	Remarks
121.4	4	0.12±0.10						a)
125.7	6	0.50±0.10	E2	1870.5	$25/2^{(-)}$	1744.8	$21/2^{(-)}$	
214.8	6	0.35±0.15						a)
278.4	18	0.45±0.15	E2	2692.1	$33/2^{+}$	2413.7	$29/2^{+}$	
283.4	6.5	-0.15±0.10	(E1)	1744.8	$21/2^{(-)}$	1461.1	$19/2^{+}$	
301.1	16	0.45±0.10	E2	2171.6	$29/2^{(-)}$	1870.5	$25/2^{(-)}$	
371.2	100	0.41±0.06	E2	547.3	$17/2^{+}$	176.1	$13/2^{+}$	
544.7	<30	0.3 ±0.2	E2	2413.7	$29/2^{+}$	1869.0	$25/2^{+}$	b)
586.2	32	0.43±0.10	(E1)	1744.8	$21/2^{(-)}$	1158.9	$21/2^{+}$	
611.6	78	0.47±0.10	E2	1158.9	$21/2^{+}$	547.3	$17/2^{+}$	
710.1	30	0.43±0.15	E2	1869.0	$25/2^{+}$	1158.9	$21/2^{+}$	
913.8	8.5	-1.05±0.20	E2/M1	1461.1	$19/2^{+}$	547.3	$17/2^{+}$	

a) Not assigned.

b) Also in ^{194}Hg.

Table 2. The γ Intensities of the 283.4 keV and 913.8 keV Lines at Various α Energies.[a)]

E_α =	34	35	40	45	47	50 MeV
I_γ (283.4 keV)	3.1	5.8	6.2	8.1	6.5	7.9±0.8
I_γ (913.8 keV)	7.3	10.9	9.8	9.9	8.5	8.5±1.0

[a)] The intensities are corrected for their angular distribution and are relative to $I_{17/2^+ \rightarrow 13/2^+} = 100$.

Table 3. Information on γ-Transitions Assigned to ^{197}Hg.

E_γ (keV)	I_γ at 34 MeV	A_2	Mult.	$E_x(i)$ (keV)	I(i)	$E_x(f)$ (keV)	I(f)	Remarks
150.7	8	0.37±0.10	E2	1833.0	$(25/2^-)$	1682.3	$(21/2^-)$	
328.6	9	0.40±0.10	E2	2161.6	$(29/2^-)$	1833.0	$(25/2^-)$	
354.1	100	0.37±0.05	E2	653.1	$17/2^+$	299.0	$13/2^+$	
408.2	<50	0.20±0.10	(E1)	1682.3	$(21/2^-)$	1274.1	$21/2^+$	a)
621.0	42	0.46±0.15	E2	1274.1	$21/2^+$	653.1	$17/2^+$	
763.1	7	0.30±0.20	E2	2037.2	$25/2^+$	1274.1	$21/2^+$	

a) Also ^{198}Pt $(2^+ \rightarrow 0^+)$.

Table 4. Information on γ-Transitions Assigned to ^{199}Hg.

E_γ (keV)	I_γ at 37 MeV	A_2	Mult.	$E_x(i)$	I(i)	$E_x(f)$	I(f)	Remarks
141.6	< 2	0.21±0.10		2629.5	$(27/2^-)$	2487.9	$(25/2^-)$	a)
155.6	2			2487.9	$(25/2^-)$	2331.9	$(21/2^-)$	
204.1	1			2629.5	$(27/2^-)$	2425.4	$(23/2^-)$	
278.1	9	0.41±0.10	E2	2766.0	$(29/2^-)$	2487.9	$(25/2^-)$	
291.4	100	0.40±0.05	E2	832.9	$17/2^+$	532.5	$13/2^+$	
380.6	20	0.51±0.15	(E1)	2487.9	$(25/2^-)$	2107.3	$25/2^+$	
438.7	6	0.2 ±0.2	(E2)	3068.2	$(31/2^-)$	2629.5	$(27/2^-)$	
522.2	⩽ 22	-0.04±0.20		2629.5	$(27/2^-)$	2107.3	$25/2^+$	a)
533.5	77	0.49±0.08	E2	1357.4	$21/2^+$	832.9	$17/2^+$	
741.5	5	-1.23±0.20	E2/M1	(1274.0	$15/2^+$)	532.5	$13/2^+$	
749.9	38	0.46±0.15	E2	2107.3	$25/2^+$	1357.4	$21/2^+$	
945.2	3	-1.03±0.20	E2/M1	1778.1	$19/2^+$	832.9	$17/2^+$	
974.5	10	0.32±0.15	(E1)	2331.9	$(21/2^-)$	1357.4	$21/2^+$	
1002.0	3	0.12±0.15						b)
1005.0	3	0.33±0.15						b)
1068.0	8	-0.49±0.15	(E1)	2425.4	$(23/2^-)$	1357.4	$21/2^+$	
1126.6	2.5	-0.77±0.20	E2/M1	2484.0	$23/2^+$	1357.4	$21/2^+$	

a) Also in ^{198}Hg.

b) Not assigned.

Table 5. Wave Functions for an $\alpha = 13/2$ and $\alpha = 11/2$ State as Expanded in Ω.

	Ω						
α	1/2	3/2	5/2	7/2	9/2	11/2	13/2
11/2	0.179	0.466	0.579	0.513	0.344	0.172	0.056
13/2	0.647	0.561	0.418	0.246	0.138	0.056	0.016

Figure Captions

Fig. 1. Gamma-ray spectra from the bombardment of a target with 60% ^{194}Pt, 30% ^{195}Pt and 10% ^{196}Pt with α particles at (a) 35 MeV and (b) 45 MeV incident energy. The spectra have been recorded with a planar Ge(Li) detector at 90° with respect to the beam. Almost all the stronger γ lines could be assigned to Hg isotopes with A = 194, 195, and 196.

Fig. 2. Gamma-ray spectra from the bombardment of a target with 60% ^{198}Pt, 30% ^{196}Pt and 10% ^{195}Pt with α particles at 34 MeV. Detection angle was 90° for the full spectrum and 45° for the insert which only shows the higher γ energies. Note that some of the lines (741.5 keV and 945.2 keV) almost vanish at 45°, they have an A_2 coefficient close to -1.0.

Fig. 3. Example of γ-γ coincidence spectra taken with a planar and a coaxial Ge(Li) detector for various transitions in ^{199}Hg. Figure 3a shows coax spectra for several gates in the planar detector and fig. 3b shows planar spectra with the gates set in the coaxial detector.

Fig. 4. Decay scheme for the low-lying high-spin states in ^{195}Hg.

Fig. 5. Decay scheme for the low-lying high-spin states in ^{197}Hg.

Fig. 6. Decay scheme for the low-lying high-spin states in ^{199}Hg.

Fig. 7. Level systematics for the low-lying high-spin states in Hg isotopes with A = 184 through A = 200. Plotted are the 0^+, 2^+, 4^+, and 6^+ quasi-rotational states in the even-even and the $13/2^+$, $17/2^+$, $21/2^+$, and $25/2^+$ decoupled states in the odd-A nuclei (solid bars) as well as the 5^-, 7^-, and 9^- and $21/2^-$, $25/2^-$ and $29/2^-$ negative-parity states (dotted lines) in the even-even and odd-A nuclei, respectively. The spectra of the odd-A

isotopes have been shifted in energy so that their isomeric $13/2^+$ states match up with the ground states in the even-even Hg isotopes. The numbers refer to the transition energies between the positive-parity states. The data on ^{191,192,193}Hg are from ref. [14]), the ones on ^{187}Hg are our own preliminary results.

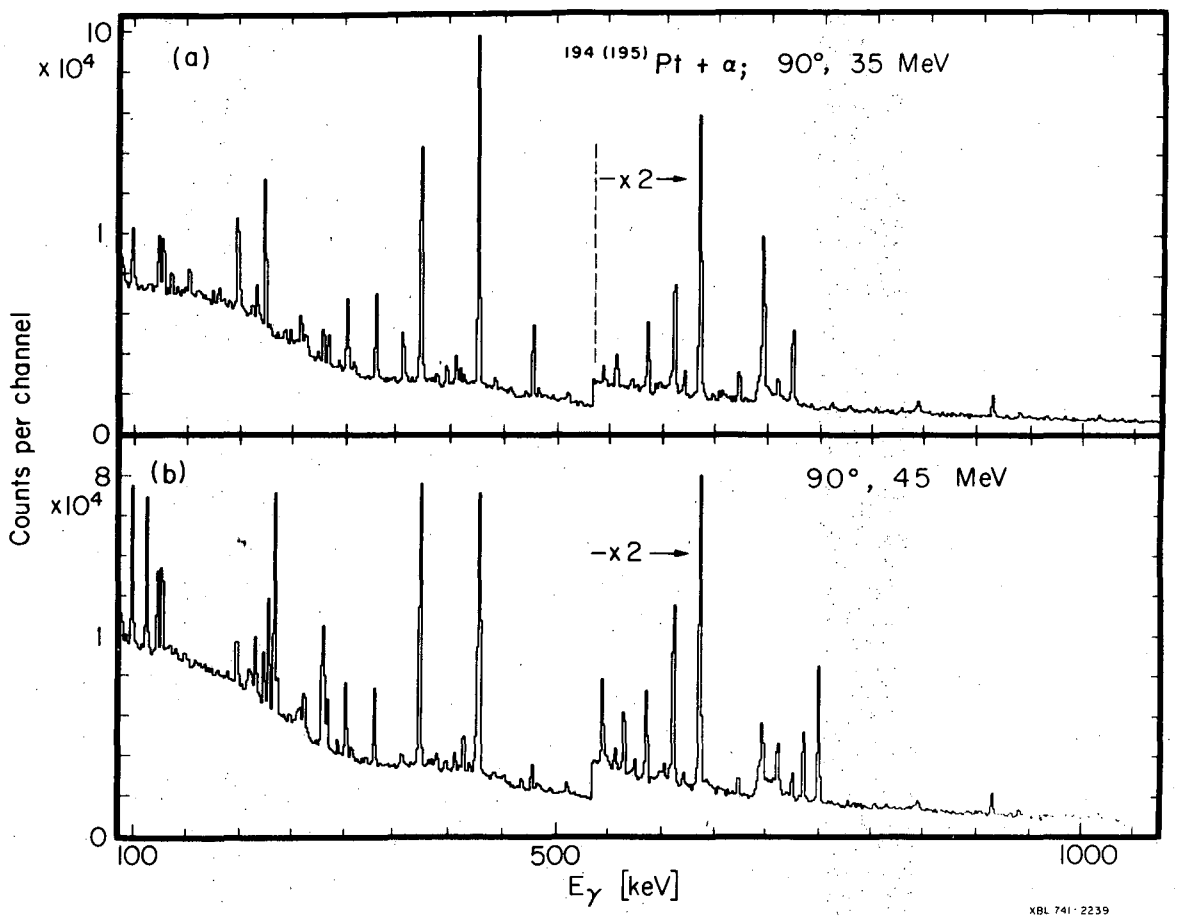
(a)
194 (195) Pt + α; 90°, 35 MeV
-x 2→
10
x 10⁴
1
0
(b)
90°, 45 MeV
-x 2→
8
x10⁴
1
0
Counts per channel
100
500
1000
Eγ [keV]
XBL 741-2239

Fig. 1

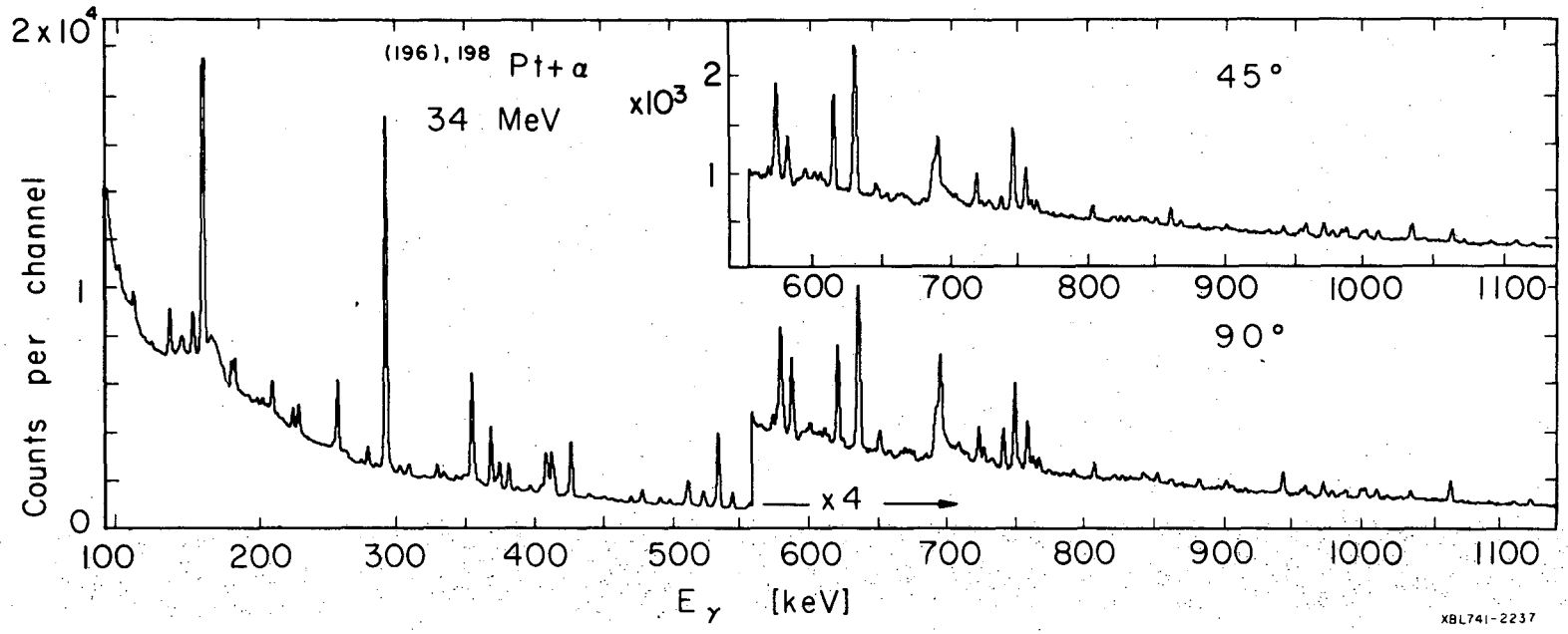
(196), 198 Pt+α
34 MeV
x10³
45°
90°
x4
Counts per channel
E γ [keV]
XBL741-2237

Fig. 2

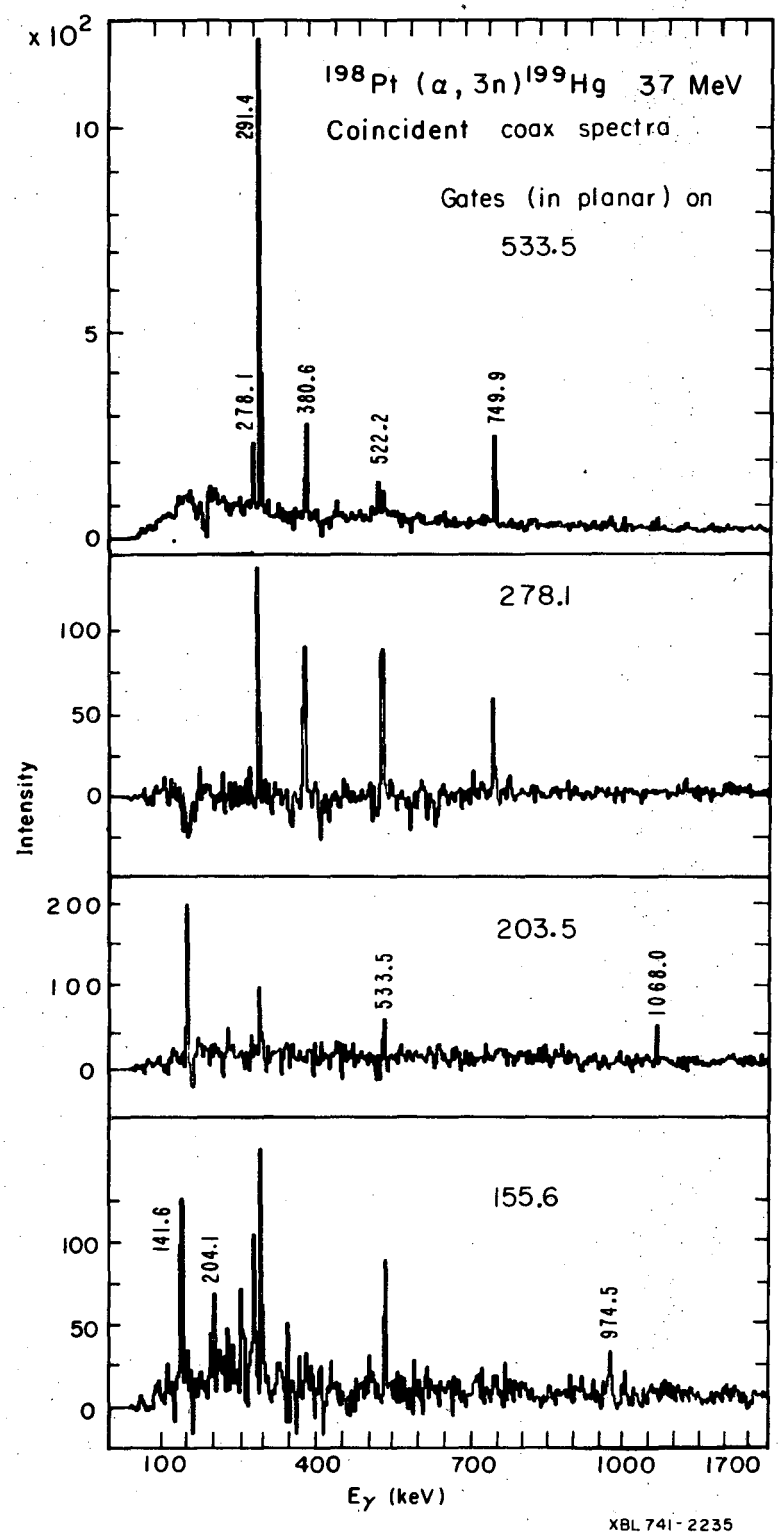
x 10²
198Pt (α, 3n)199Hg 37 MeV
Coincident coax spectra
Gates (in planar) on
533.5
291.4
278.1
380.6
522.2
749.9
278.1
203.5
533.5
1068.0
155.6
141.6
204.1
974.5
Intensity
Eγ (keV)
XBL 741-2235

Fig. 3a

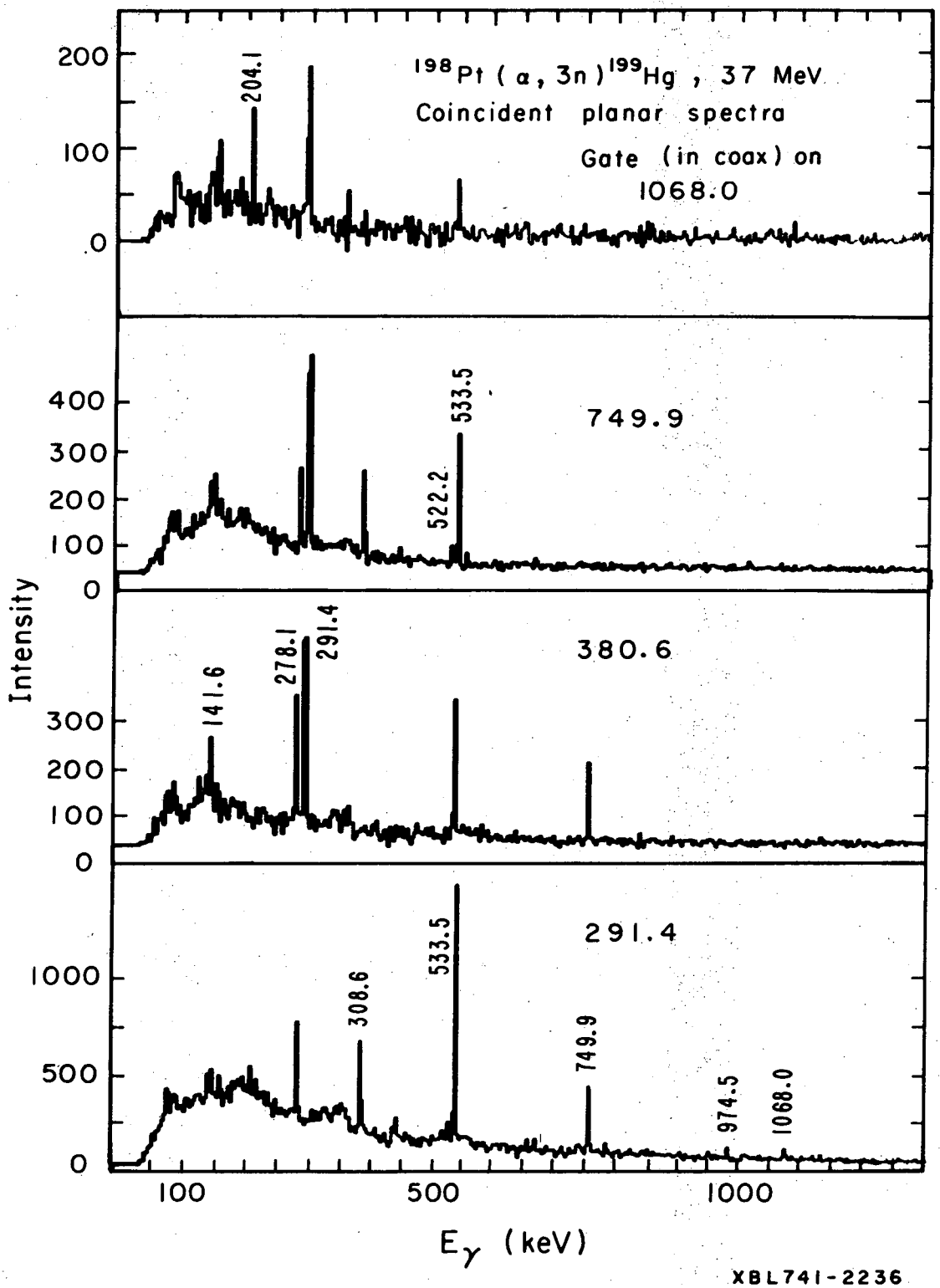
^{198}Pt (α, 3n)^{199}Hg , 37 MeV
Coincident planar spectra
Gate (in coax) on
1068.0
204.1
749.9
533.5
522.2
380.6
141.6
278.1
291.4
291.4
533.5
308.6
749.9
974.5
1068.0
Intensity
E_γ (keV)
XBL741-2236

Fig. 3b

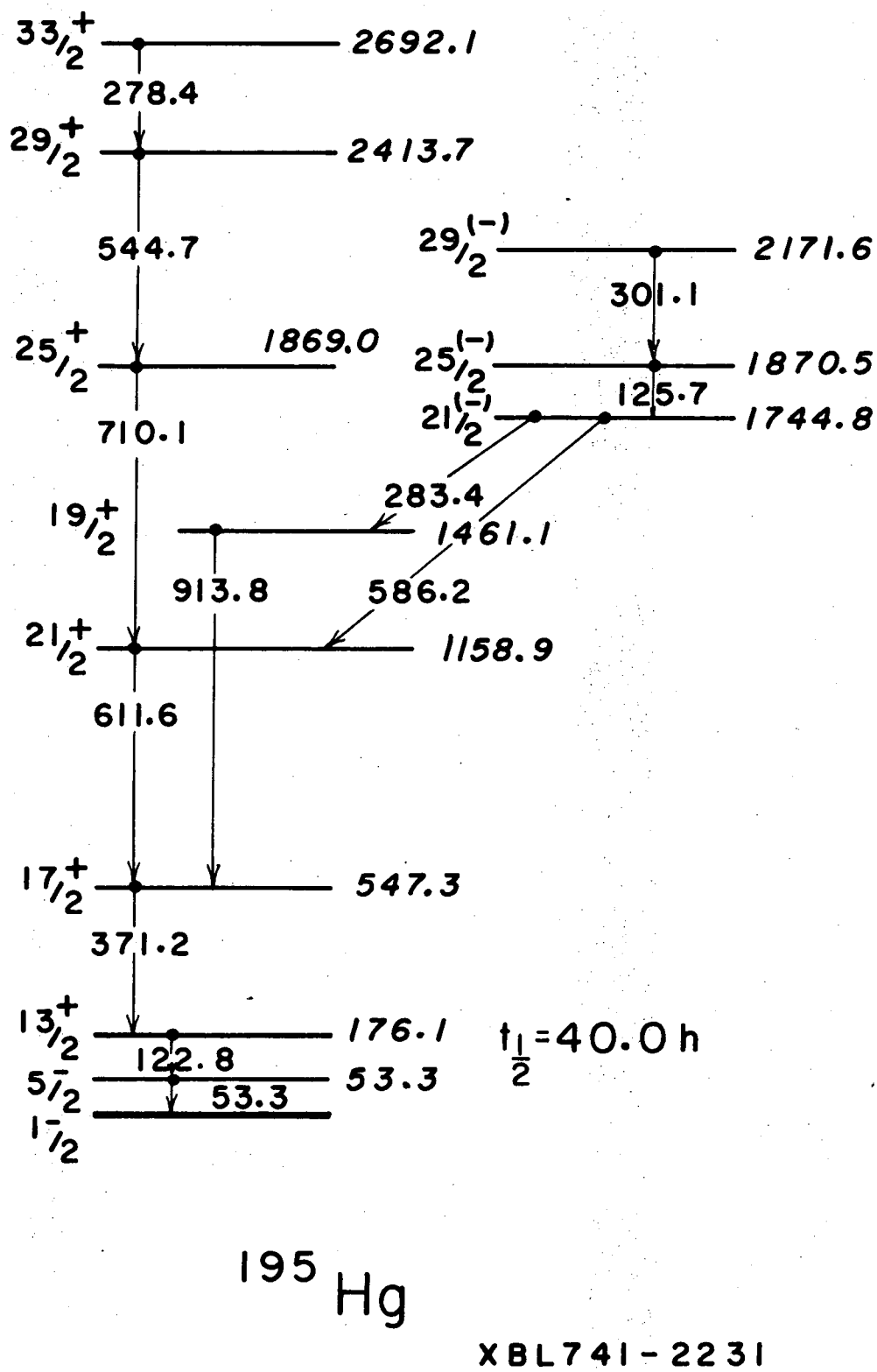
33/2+
2692.1
278.4
29/2+
2413.7
544.7
29/2(-)
2171.6
301.1
25/2+
1869.0
25/2(-)
1870.5
125.7
21/2(-)
1744.8
710.1
283.4
19/2+
1461.1
913.8
586.2
21/2+
1158.9
611.6
17/2+
547.3
371.2
13/2+
176.1
t1/2=40.0 h
122.8
5/2-
53.3
53.3
1/2-
195 Hg
XBL741-2231

Fig. 4

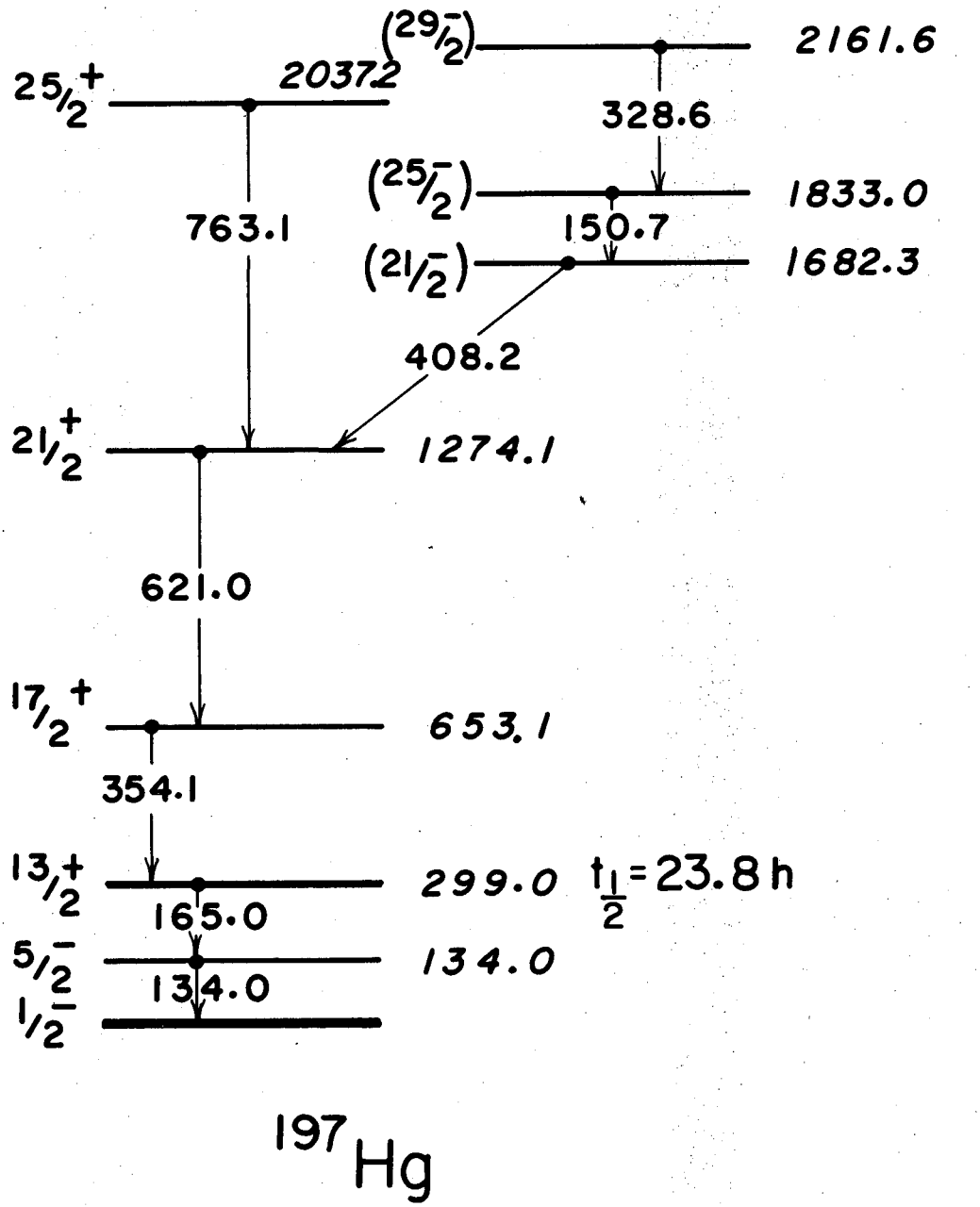

XBL741-2232

Fig. 5

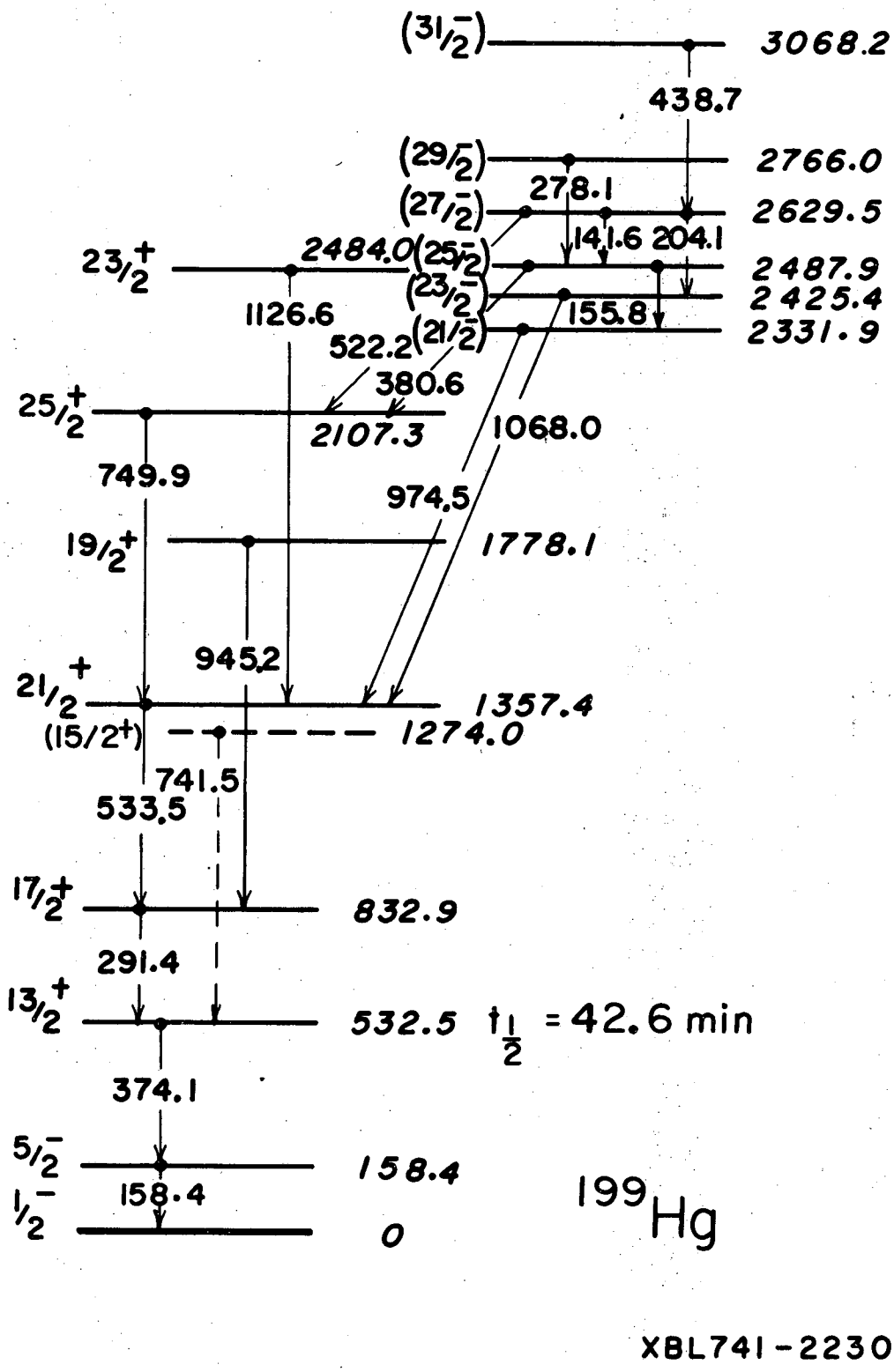
(31/2⁻)
3068.2
438.7
(29/2⁻)
2766.0
278.1
(27/2⁻)
2629.5
141.6
204.1
23/2⁺
2484.0
(25/2⁻)
2487.9
(23/2⁻)
2425.4
1126.6
155.8
(21/2⁻)
2331.9
522.2
380.6
25/2⁺
2107.3
1068.0
749.9
974.5
19/2⁺
1778.1
945.2
21/2⁺
1357.4
(15/2⁺)
1274.0
741.5
533.5
17/2⁺
832.9
291.4
13/2⁺
532.5
t1/2 = 42.6 min
374.1
5/2⁻
158.4
158.4
1/2⁻
0
199Hg
XBL741-2230

Fig. 6

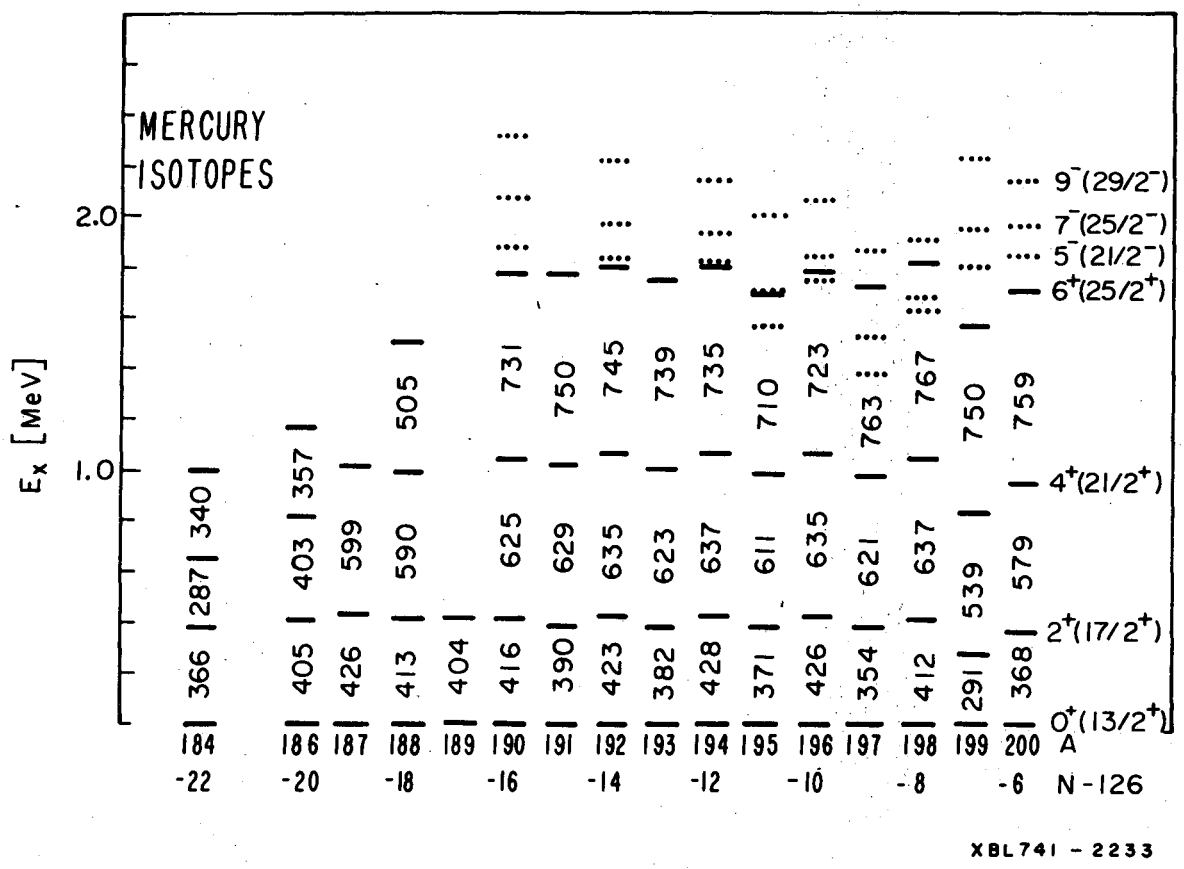
MERCURY
ISOTOPES
E_x [MeV]
2.0
1.0
9⁻(29/2⁻)
7⁻(25/2⁻)
5⁻(21/2⁻)
6⁺(25/2⁺)
4⁺(21/2⁺)
2⁺(17/2⁺)
0⁺(13/2⁺)
184 186 187 188 189 190 191 192 193 194 195 196 197 198 199 200 A
-22 -20 -18 -16 -14 -12 -10 -8 -6 N-126
366 287 340
405 403 357
426 599
413 590 505
404
416 625 731
390 629 750
423 635 745
382 623 739
428 637 735
371 611 710
426 635 723
354 621 763
412 637 767
291 539 750
368 579 759
XBL741 - 2233

Fig. 7

LEGAL NOTICE

This report was prepared as an account of work sponsored by the United States Government. Neither the United States nor the United States Atomic Energy Commission, nor any of their employees, nor any of their contractors, subcontractors, or their employees, makes any warranty, express or implied, or assumes any legal liability or responsibility for the accuracy, completeness or usefulness of any information, apparatus, product or process disclosed, or represents that its use would not infringe privately owned rights.

TECHNICAL INFORMATION DIVISION
LAWRENCE BERKELEY LABORATORY
UNIVERSITY OF CALIFORNIA
BERKELEY, CALIFORNIA 94720